2392 *Inorg. Chem.* **2010**, *49*, 2392–2397
DOI: 10.1021/ic9022882

Inorganic Chemistry
Article

Novel Layered Hybrid Fluoroaluminate in the Composition Space Diagram of the $Al(OH)_3$-H*gua*Cl-HF_{aq}-EtOH System

Karim Adil, Armel Le Bail, Marc Leblanc, and Vincent Maisonneuve*

Laboratoire des Oxydes et Fluorures, UMR CNRS 6010, Faculté des Sciences et Techniques, Université du Maine, Avenue Olivier Messiaen, 72085 Le Mans Cedex 09, France

Received November 18, 2009

A composition space diagram is used to establish the stability regions of hybrid fluoroaluminates synthesized by solvothermal reactions in the $Al(OH)_3$−H*gua*Cl−HF_{aq}−EtOH system. The syntheses are conducted using microwave heating at 190 °C for 1 h. The structures of two new guanidinium fluoroaluminates, $(H_3O)_2\cdot[Hgua]_{16}\cdot(Al_4F_{18})_3\cdot H_2O$ and $[Hgua]_2\cdot(Al_5F_{17})$, are reported. $(H_3O)_2\cdot[Hgua]_{16}\cdot(Al_4F_{18})_3\cdot H_2O$, determined from single-crystal X-ray data, consists of discrete $(Al_4F_{18})^{6-}$ polyanions, while $[Hgua]_2\cdot(Al_5F_{17})$, solved from powder X-ray diffraction data in direct space, contains unprecedented Al_5F_{17} layers constructed from the intergrowth of HTB and perovskite columns. A disorder of H_2O and H_3O^+ is evidenced in $(H_3O)_2\cdot[Hgua]_{16}\cdot(Al_4F_{18})_3\cdot H_2O$ together with a disorder of guanidinium cations in the interlayer space of $[Hgua]_2\cdot(Al_5F_{17})$.

Introduction

The solvothermal reaction of inorganic reagents with amines and aqueous acids under subcritical conditions (T < 500 K and P < 100 bar) is well-known to be the leading technique for organic−inorganic material elaboration. During the past decade, the uncountable combinations led to numerous hybrid compounds, which belong to the metal oxide class, with structural inorganic architectures ranging from molecular to three-dimensional (3D). This continued interest, especially for materials with open frameworks, is driven by expected applications such as catalysis, ion exchange, separation, or gas storage.[1,2] In contrast, the research activity in the solvothermal chemistry of metal fluorides is weak. The list of hybrid fluorides with purely fluorinated inorganic layers is relatively limited. That with a 3D inorganic network is even more restricted; only four compounds are reported (Table 1).

Our current work is focused on the hybrid fluoride chemistry, specifically with aluminum. For example, the recent investigation of the Al_2O_3−*tren*−HF_{aq}−ethanol (EtOH) system at 190 °C revealed more than 18 hybrid fluoroaluminates that are built up from isolated inorganic polyanions $(AlF_6)^{3-}$,[3] $(Al_2F_{10})^{4-}$,[4] $(Al_4F_{18})^{6-}$,[5] $(Al_7F_{30})^{9-}$,[6] and $(Al_8F_{35})^{11-}$,[7] or infinite inorganic chains such as Al_7F_{29}[6] and Al_6F_{24};[8] most of these entities were unknown. However, these phases have a low dimensionality, limited to one-dimensional (1D). To study the chemical systems, we apply the concept of compositional space diagrams.[9,10] Although the representation of the compositional space diagrams is similar to that of phase diagrams, important differences exist. Only the crystallized solid products are analyzed. Consequently, the amorphous products and/or solution species are neglected. The domain limits are visually estimated, and mixtures of crystallized phases are systematically found at the vicinity of the limits. Nevertheless, compositional space diagrams, which precisely fit the stability domains of crystalline solids, are useful in the synthesis of the compounds in a phase-pure form. Because of the very short time of synthesis (1 h), microwave heating is applied. This route offers the advantage of exploring a diagram on large-concentration domains. Moreover, large quantities of pure powders can be obtained and single crystals frequently grow.

Herein, we report on the microwave-heating-assisted solvothermal synthesis in the $Al(OH)_3$−H*gua*Cl−HF_{aq}−EtOH system at 190 °C for 1 h and the structural characterization

*To whom correspondence should be addressed. E-mail: vincent.maisonneuve@univ-lemans.fr. Tel.: +33 2 4383 3561. Fax: +33 2 4383 3506.

(1) Meier, W. H.; Olson, D. H. *Atlas of Zeolite Structure Types*; Butterworth-Heinemann: London, 1992.
(2) Ertl, G., Knözinger, H., Weitkamp, J., Eds. *Handbook of Heterogeneous Catalysis*; VCH: Berlin, 1997.
(3) Adil, K.; Ben Ali, A.; Leblanc, M.; Maisonneuve, V. *Solid State Sci.* **2006**, *8*, 698.
(4) Adil, K.; Leblanc, M.; Maisonneuve, V. *Acta Crystallogr.* **2004**, *E60*, m1319.
(5) Adil, K.; Leblanc, M.; Maisonneuve, V. *J. Fluorine Chem.* **2006**, *127*, 1349.
(6) Goreshnik, E.; Maisonneuve, V.; Leblanc, M. *Z. Anorg. Allg. Chem.* **2002**, *628*, 162.
(7) Adil, K.; Leblanc, M.; Maisonneuve, V. *J. Fluorine Chem.* **2010**, *130*, 1099−1105.
(8) Adil, K.; Courant, S.; Marrot, J.; Leblanc, M.; Maisonneuve, V. *Solid State Sci.* **2007**, *9*, 531.
(9) Halasyamani, P.; Willis, M. J.; Stern, C. L.; Lundquist, P. M.; Wong, G. K.; Poeppelmeier, K. R. *Inorg. Chem.* **1996**, *35*, 1367.
(10) Norquist, A. J.; Heier, K. R.; Stern, C. L.; Poeppelmeier, K. R. *Inorg. Chem.* **1998**, *37*, 6495.

Published on Web 02/04/2010

Table 1. Hybrid Fluorides with Purely Fluorinated Inorganic Layers (2D) or Frameworks (3D)

layers (2D)	frameworks (3D)
$[Hpy]\cdot(Al_3F_{10})$[22]	$[Hmeam]\cdot(Li_2Be_2F_7)$[34]
$[H_2en]\cdot(Li_2Be_2F_8)$[23]	$[H_2en]_{0.5}\cdot(Y_2F_7)$[35]
$[Hmeam]_2\cdot(Li_2Be_2F_8)\cdot 2H_2O$[23]	$[H_2dap]_{0.5}\cdot(Y_3F_{10})$[36]
$[C_6H_4(CH_3)CH_2NH_3]\cdot(LiBeF_4)$[24]	$(H_3O)\cdot[Hgua]_5\cdot(ZrF_5)_6$[37]
$[C_6H_4(Cl)CH_2NH_3]\cdot(LiBeF_4)$[24]	
$[H_2dap]\cdot(LiBeF_4)_2$[24]	
$[C_6H_5(CH_2)_3NH_3]\cdot(LiBeF_4)$[24]	
$[H_2pipz]_2\cdot(Mn_4F_{16})$[25]	*dap* = 1,3-diaminopropane
$[H_2en]\cdot(Sc_2F_8)$[26]	*dab* = 1,4-diaminabutane
$[H_2pipz]_{0.5}\cdot(ThF_5)$[27]	*dah* = 1,6-diaminohexane
$[H_2en]\cdot(M_2F_{10})$ (M = Ce,[28] U,[29] Np[30])	*en* = ethylenediamine
$[H_2dap]\cdot(U_2F_{10})\cdot 2H_2O$[31]	*gua* = guanidine
$[H_2dab]\cdot(U_2F_{10})\cdot 3H_2O$[31]	*meam* = methylamine
$[H_2dah]\cdot(U_2F_{10})\cdot 2H_2O$[31]	*pipz* = piperazine
$[H_4tren]\cdot(U_5F_{24})$[31]	*py* = pyridine
$[H_2en]\cdot(Zr_2F_{10})\cdot H_2O$[32]	*tren* = tris(2-aminoethyl)-amine
$[H_2dap]\cdot(Zr_2F_{10})\cdot H_2O$[33]	
$[Hmeam]_2\cdot(Zr_2F_{10})\cdot H_2O$[33]	

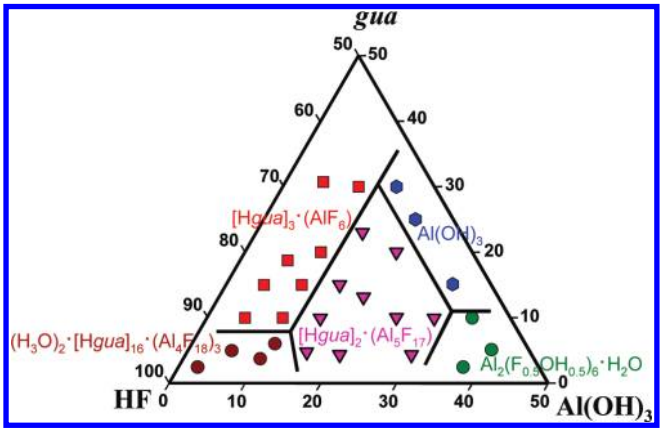

Figure 1. Compositional space diagram of the $Al(OH)_3$–H*gua*Cl–HF_{aq}–EtOH system at 190 °C and $[Al^{3+}] = 0.4$ mol L^{-1} ($Al_2[(OH)_{0.5}F_{0.5}]_6\cdot H_2O$ = pyrochlore).

of two new guanidine (*gua*)-templated aluminum fluorides. $(H_3O)_2\cdot[Hgua]_{16}\cdot(Al_4F_{18})_3\cdot H_2O$ shows isolated $(Al_4F_{18})^{6-}$ polyanions, while $[Hgua]_2\cdot(Al_5F_{17})$ contains a 2D architecture with an unprecedented perovskite–HTB-related layer.

Experimental Section

The composition space diagram was constructed for the $Al(OH)_3$–H*gua*Cl–HF_{aq}–EtOH system from approximately 30 separate reactions and a constant aluminum concentration $[Al^{3+}] = 0.4$ mol L^{-1} (Figure 1). All reactions were performed from a mixture of $Al(OH)_3$ (Merk), guanidinium chloride noted as H*gua*Cl (Aldrich), a hydrofluoric acid solution (40% HF, Prolabo), and EtOH. $Al(OH)_3$ and HF_{aq} were first loaded into a poly(tetrafluoroethylene)-lined autoclave. After a quick stirring, EtOH and guanidinium chloride were then added, and the solvothermal reactions are performed at 190 °C in a microwave oven (CEM 2100) for 1 h. After natural cooling to room temperature, the solid products were washed with EtOH and dried at room temperature. All samples were characterized by powder X-ray diffraction (XRD) on a PANALYTICAL MPDPRO diffractometer (geometry Bragg–Brentano) equipped with a linear X'celerator detector.

Thermogravimetric analyses were performed with a TA Instruments SDT-Q600 with a heating rate of 10 °C min^{-1} and in the temperature range 25–1200 °C. Under an air atmosphere, hydrolysis occurred above 600 °C to give Al_2O_3; the total weight losses were in good agreement with the expected values: expt/theor = 74.1/71.4 for $(H_3O)_2\cdot[Hgua]_{16}\cdot(Al_4F_{18})_3\cdot H_2O$ and 55.9/58.7 for $[Hgua]_2\cdot(Al_5F_{17})$.

Aluminum (inductively coupled plasma) and fluorine (ion-specific electrode) elemental analyses (expt/calcd) of $(H_3O)_2\cdot[Hgua]_{16}\cdot(Al_4F_{18})_3\cdot H_2O$ [Al 12.6(3)/13.7; F 41.8(9)/43.3] and of $[Hgua]_2\cdot(Al_5F_{17})$ [Al 23.0(6)/23.3 and F 40.0(9)/55.9] suggest a F/OH substitution for $[Hgua]_2\cdot(Al_5F_{17})$.

Perkin-Elmer Spectrum One equipped with a diamond ATR was used for IR spectroscopy (450–4000 cm^{-1}). Both compounds exhibit very strong bands at 1680 and 3200–3500 cm^{-1} because of characteristic ν_{CN} and ν_{NH} vibrations of the guanidinium cations, respectively. A broad and weak band around 2800 cm^{-1} is observed for $(H_3O)_2\cdot[Hgua]_{16}\cdot(Al_4F_{18})_3\cdot H_2O$ and could correspond to the ν_{OH} vibrational frequency of the hydronium cations.

An optical test of second harmonic generation (SHG) was performed on both phases. Opposite from $[Hgua]_2\cdot(Al_5F_{17})$, a signal, significant for noncentrosymmetry, was observed for $(H_3O)_2\cdot[Hgua]_{16}\cdot(Al_4F_{18})_3\cdot H_2O$.

The structure of $(H_3O)_2\cdot[Hgua]_{16}\cdot(Al_4F_{18})_3\cdot H_2O$ was solved from single-crystal X-ray data collected on a Bruker APEX II CCD diffractometer [Bruker Triumph monochromator Mo Kα (λ = 0.710 69 Å)] at 150 K. The structure solution was found by direct methods (TREF option) and extended by Fourier maps and subsequent refinements (*SHELXS-97* and *SHELXL-97*[11] programs included in the *WINGX* package[12]). All non-hydrogen atoms were refined anisotropically, whereas hydrogen atoms of the $[Hgua]^+$ cations were geometrically constrained (HFIX option).

In the absence of single crystals of $[Hgua]_2\cdot(Al_5F_{17})$, a powder pattern was recorded in Bragg–Brentano geometry with a Bruker D8-Advance diffractometer equipped with a diffracted beam graphite monochromator (radiation Cu Kα). A C-centered orthorhombic cell was obtained from the McMaille indexing software [M(20) = 30; F(20) = 43].[13] This cell was confirmed by a satisfying whole powder pattern fit by the Le Bail method[14] using the *Fullprof* software.[15] However, a few additional intense peaks with larger broadening could only be explained by the presence of a cubic-phase $AlF_3\cdot H_2O$ (a = 3.61 Å).[16] Several experiments allowed a reduction of the presence of the cubic phase, varying the HF–*gua* ratio. The extracted intensities from the best powder pattern, retaining the *Cmmm* space group, were used for the structure solution by direct space methods (*ESPOIR* software[17]); two rotating and translating independent AlF_6 octahedra and one CN_3 group were used in a Monte Carlo process, until $R \sim 15\%$. The octahedra were found to be connected by corners, forming layers parallel to the *bc* plane. Then, Rietveld[18] refinements led to a good fit, as shown in Figure 2. In order to obtain satisfying C–N and N–N distances, the geometry of the CN_3 group was constrained to be a carbon-centered nitrogen triangle (hydrogen atoms were not located). However, the thermal parameter of the N1 atom remained very high, indicating a disorder or a lower symmetry. Attempts to obtain better results in *Cmm*2 and *C*222 space groups failed. This fact is in agreement with the negative test of SHG. With such a high thermal parameter, there even is doubt about the presence of the atom; however,

(11) Sheldrick, G. M. *Appl. Crystallogr.* **2008**, *A64*, 112.
(12) Farrugia, L. J. *J. Appl. Crystallogr.* **1999**, *32*, 837.
(13) Le Bail, A. *Powder Diffr.* **2004**, *19*, 249.
(14) Le Bail, A. *Powder Diffr.* **2005**, *20*, 316.
(15) Rodriguez-Carvajal, J. *Physica B* **1993**, *192*, 55.
(16) Chandross, R. *Acta Crystallogr.* **1964**, *17*, 1477.
(17) Le Bail, A. *Mater. Sci. Forum* **2001**, *378–381*, 65.
(18) Rietveld, H. M. *J. Appl. Crystallogr.* **1969**, *2*, 65.

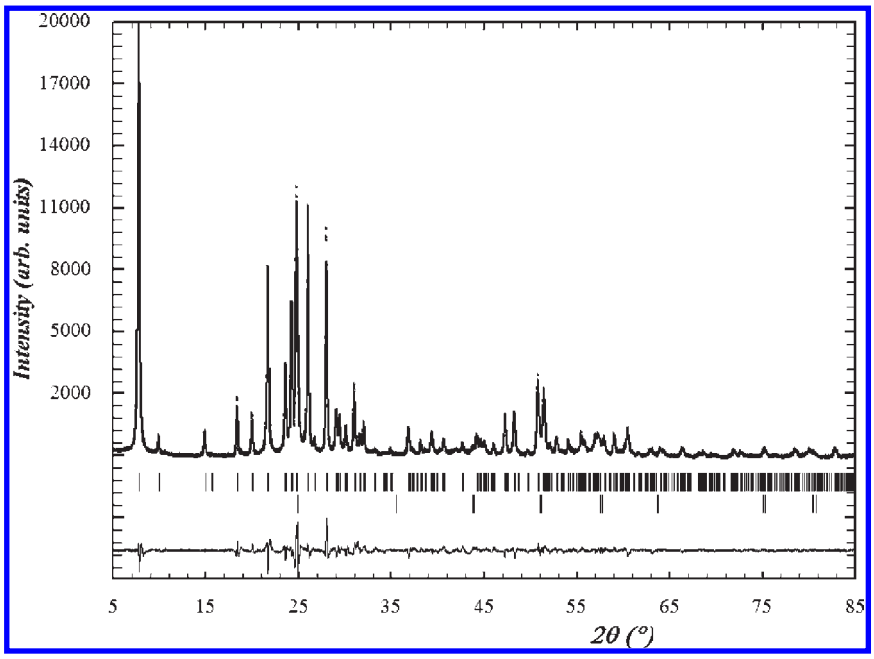

Figure 2. Final profile refinement of $[Hgua]_2\cdot(Al_5F_{17})$: observed (line), calculated (point), and difference (bottom) profiles of XRD data. Vertical bars are related to the calculated Bragg reflection positions (lower second raw = $AlF_3\cdot H_2O$).

Table 2. Crystallographic Data of $(H_3O)_2\cdot[Hgua]_{16}\cdot(Al_4F_{18})_3\cdot H_2O$ and $[Hgua]_2\cdot(Al_5F_{17})$

compound	$(H_3O)_2\cdot[Hgua]_{16}\cdot(Al_4F_{18})_3\cdot H_2O$	$[Hgua]_2\cdot(Al_5F_{17})$
formula	$Al_{12}F_{54}O_3N_{48}C_{16}H_{104}$	$Al_5F_{17}N_6C_2H_{12}$
fw (g mol^{-1})	2367.02	578.04
	single crystal	powder
diffractometer	Bruker APEX II CCD	Bruker D8-Advance
monochromator, wavelength (Å)	Bruker Triumph, 0.710 73	−, 1.540 56
cryst syst, space group	cubic, $I\bar{4}3d$	orthorhombic, *Cmmm*
a (Å)	20.465(1)	22.609(1)
b (Å)		9.638(1)
c (Å)		3.593(1)
V (Å^3), *Z*	8571.1(7), 4	783.0(1), 2
ρ_{calcd}, ρ_{expt} (g cm^{-3})	1.834, 1.83(1)	2.45, 2.30(1)
2θ range (deg), temperature (K)	3−60, 150	3−90, 293
reflns measd/unique/ [$I > 2\sigma(I)$]	78214/4651/1850	
(*hkl*) limits	$-16 \le h \le 16$, $-28 \le k \le 28$, $-29 \le l \le 29$	
refined param	107	
R1, wR2, GOF (F^2)	0.0555, 0.189, 0.978	
$\Delta\rho_{min}$, $\Delta\rho_{max}$ (e Å^{-3})	−0.43, 0.83	
Flack parameter	0.0(5)	
no. of indep reflns		218
no. of intensity-dependent param		82
distance restraints		4
R_P, R_{wp}		0.12, 0.130
R_B, R_F		0.034, 0.030

its removal produces an increase of the Bragg *R* factor from 3.4 to 12.4%, which is not really surprising in a structure in which all atoms are light X-ray scatterers (Al^{3+} and F^- ions being isoelectronic). No clue for a symmetry lowering to the monoclinic symmetry can be found from the powder pattern. It must be noted that anisotropic line broadening for (*h*00) and (*hkl*) peaks with large *h* values was detected but not accounted for during the Rietveld refinements. This anisotropic broadening suggests crystallite size effects and/or stacking faults along the *a* axis; these effects are expected from the two-dimensional (2D) character of the structure and are probably exalted by a F/OH substitution.

Table 3. Selected Interatomic distances (Å) in $(H_3O)_2\cdot[Hgua]_{16}\cdot(Al_4F_{18})_3\cdot H_2O$

Al1−F4	1.767(3)	C1−N1	1.324(5)
Al1−F1	1.772(3)	C2−N3	1.293(9)
Al1−F2	1.777(3)	C2−N2	1.339(8)
Al1−F5	1.829(2)	C2−N4	1.363(8)
Al1−F3	1.837(3)		
Al1−F3	1.855(3)		

Table 4. Selected Interatomic Distances (Å) in $[Hgua]_2\cdot(Al_5F_{17})$

Al1−F1	2 × 1.80(1)	C−N1	1.33(1)
Al1−F2	1.70(1)	C−N2	1.30(1)
Al1−F3	1.82(1)		
Al1−F4	1.80(1)	N1−F2	2 × 2.83(1)
Al1−F5	1.82(1)	N2−F2	4 × 3.23(1)
Al2−F3	4 × 1.82(1)		
Al2−F6	2 × 1.80(1)		

The details of the structure determinations are given in Table 2. The main bond lengths are given in Tables 3 and 4.

Crystallographic data (excluding structure factors) for the structures in this paper have been deposited with the Cambridge Crystallographic Data Centre as supplementary publication nos. CCDC 729488 ($(H_3O)_2\cdot[Hgua]_{16}\cdot(Al_4F_{18})_3\cdot H_2O$) and 729489 $[Hgua]_2\cdot(Al_5F_{17})$. Copies of the data can be obtained, free of charge, upon application to CCDC, 12 Union Road, Cambridge CB2 1EZ, U.K. (fax +44 1223 336033 or e-mail deposit@ccdc.cam.ac.uk).

Results

The compositional space diagram for $Al(OH)_3$−*Hgua*Cl−HF_{aq}−EtOH is shown in Figure 1. The labels, associated with the composition of the solids, are located at the figurative points of the starting compositions. The objective of preparing new dense hybrid fluorides led to exploration of the high HF concentration part of the composition space. Five distinct crystallization fields appear in this system at 190 °C and $[Al^{3+}] = 0.4$ mol L^{-1}. The inorganic hydroxyfluoride

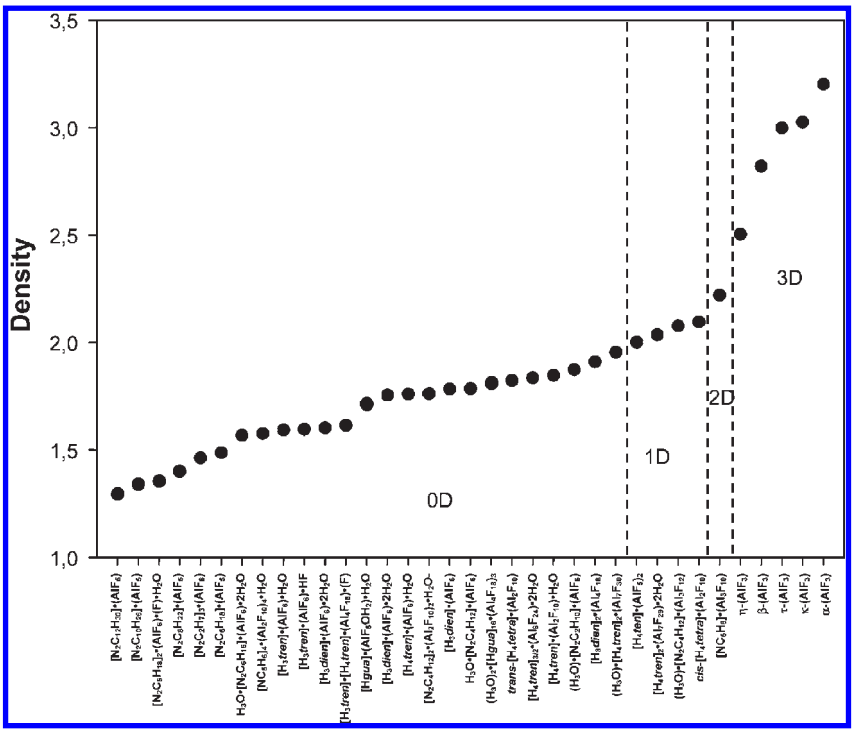

Figure 3. Densities of known hybrid aluminum fluorides and five forms of AlF_3. The regions separated by the dotted lines are related to the inorganic sublattice dimensionality.

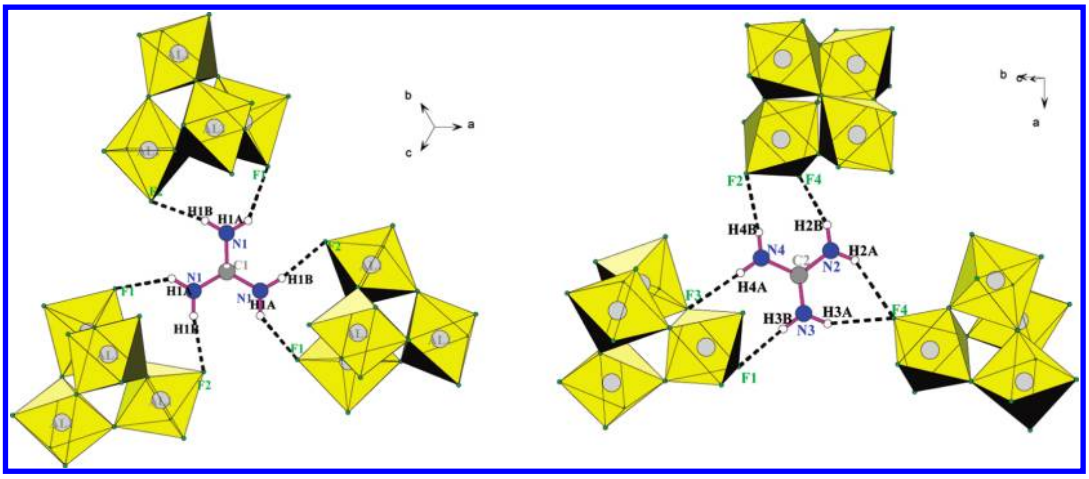

Figure 4. Hydrogen bonds between the $[Hgua]^+$ cations and the $(Al_4F_{18})^{6-}$ polyanions in $(H_3O)_2 \cdot [Hgua]_{16} \cdot (Al_4F_{18})_3 \cdot H_2O$.

pyrochlore $Al_2(F_{0.5},OH_{0.5})_6 \cdot H_2O$[19] crystallizes at low HF and guanidine concentrations, below 0.6 and 0.1 mol L^{-1}, respectively. At [HF] < 1.5 mol L^{-1} and 0.2 mol L^{-1} < [H*gua*Cl] < 0.8 mol L^{-1}, no reaction occurs and only the metallic precursor $Al(OH)_3$ gibbsite[20] subsists. The last three regions are dominated by $[Hgua]_3 \cdot (AlF_6)$, $(H_3O)_2 \cdot [Hgua]_{16} \cdot (Al_4F_{18})_3 \cdot H_2O$ and $[Hgua]_2 \cdot (Al_5F_{17})$. $[Hgua]_3 \cdot (AlF_6)$, previously reported,[21] exists at [H*gua*Cl] > 0.2 mol L^{-1} and at intermediate HF concentration (2.4 ≤ [HF] ≤ 6.8 mol L^{-1}). $(H_3O)_2 \cdot [Hgua]_{16} \cdot (Al_4F_{18})_3 \cdot H_2O$ is present at high HF concentration (4.5 mol L^{-1} ≤ [HF] ≤ 15.5 mol L^{-1}). The surface of the crystallization zone of $[Hgua]_2 \cdot (Al_5F_{17})$, located in the center of the represented composition space diagram, is large.

(19) Fourquet, J.-L.; Rivière, M.; LeBail, A.; Nygrens, M.; Grins, J. *Eur. J. Solid State Inorg. Chem.* **1988**, *25*, 535.
(20) Saalfeld, H.; Wedde, M. *Z. Kristallogr., Kristallgeom., Kristallphys., Kristallchem.* **1974**, *139*, 129.
(21) Grottel, M.; Kozak, A.; Maluszynska, H.; Pajak, Z. *J. Phys.: Condens. Matter* **1992**, *4*, 1837.
(22) Harlow, R. L.; Herron, N.; Li, Z.; Vogt, T.; Solovyov, L.; Kirik, S. *Chem. Mater.* **1999**, *11*, 2562.
(23) Gerrard, L. A.; Weller, M. T. *J. Chem. Soc., Dalton Trans.* **2002**, *23*, 4402.
(24) Gerrard, L. A.; Weller, M. T. *Chem.—Eur. J.* **2003**, *9*, 4936.
(25) Stief, R.; Massa, W. *Z. Anorg. Allg. Chem.* **2006**, *632*, 797.
(26) Stephens, N. F.; Slawin, A. M. Z.; Lightfoot, P. *Chem. Commun.* **2004**, 614.
(27) Kim, J. Y.; Norquist, A. J.; O'Hare, D. *Chem. Commun.* **2002**, 2198.
(28) Sykora, R. E.; Albrecht-Schmitt, T. E. *Chem. Mater.* **2001**, *13*, 4399.
(29) Almond, P. M.; Deakin, L.; Porter, M. J.; Mar, A.; Albrecht-Schmitt, T. E. *Chem. Mater.* **2000**, *12*, 3208.
(30) Sullens, T. A.; Almond, P. M.; Albrecht-Schmitt, T. E. *Acta Crystallogr.* **2004**, *E60*, m973.
(31) Francis, R. J.; Halasyamani, P. S.; O'Hare, D. *Chem. Mater.* **1998**, *10*, 3131.
(32) Sykora, R. E.; Ruf, M.; Albrecht-Schmitt, T. E. *J. Solid State Chem.* **2001**, *159*, 198.

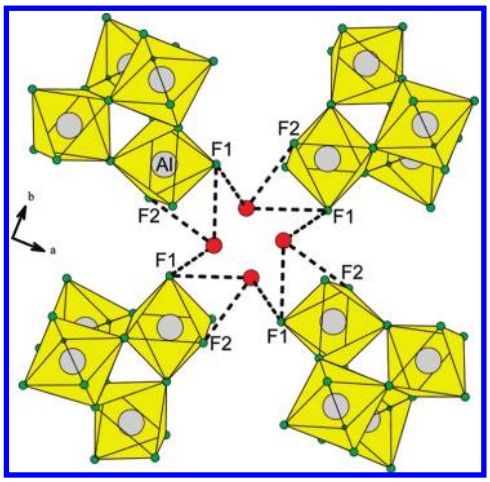

Figure 5. Hydrogen bonds between the H_3O^+ cations or H_2O and the $(Al_4F_{18})^{6-}$ polyanions in $(H_3O)_2 \cdot [Hgua]_{16} \cdot (Al_4F_{18})_3 \cdot H_2O$.

in two sets; the short and long distances correspond to terminal and bridging fluorine atoms, respectively. The Al−Al distances (3.50 and 3.52 Å) and Al−Al−Al angles (59.59 and 60.21°) in this tetrameric entity, already observed in $[H_3dien]_2 \cdot (Al_4F_{18})$,[5] are close to ideal. One out of two crystallographically independent guanidinium cations possesses an ideal ternary symmetry (Figure 4, left). However, all guanidinium environments, constituted by three $(Al_4F_{18})^{6-}$ polyanions, are similar (Figure 4), with average F···H distances of 2.15 Å. A total of 12 oxygen atoms occupy statistically the 48e sites; the electroneutrality is satisfied when eight oxygen atoms are attributed to the hydronium cations and four to the water molecules. A network of hydrogen bonds establishes itself between these H_2O molecules or the H_3O^+ cations and the tetrameric entities (Figure 5).

In $[Hgua]_2 \cdot (Al_5F_{17})$, no geometrical restraints on the AlF_6 octahedra were applied during the refinements. Nevertheless, the average Al−F interatomic distance is close to the expected value (1.81 Å), with the exception of the too short

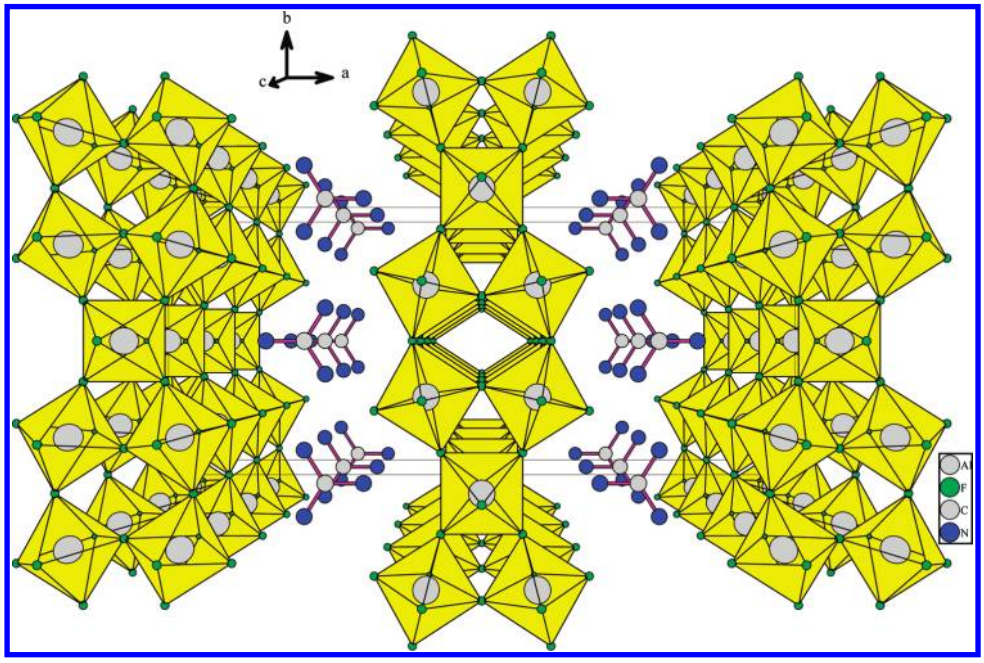

Figure 6. [001] projection of $[Hgua]_2 \cdot (Al_5F_{17})$.

Several attempts to grow crystals were performed by both classical (Parr autoclaves) and microwave-heating methods; however, only powders were obtained. Before the structural determination was started, the interest of this phase was evaluated by considering its density. Figure 3, gathering all known hybrid fluoroaluminates, indicates clearly a correlation between the density and the dimensionality of the inorganic network. The experimental density of $[Hgua]_2 \cdot (Al_5F_{17})$ (2.10), intermediate between 1D and 3D fluoroaluminates, suggested a formulation with 2D inorganic layers.

Discussion

Two new hybrid aluminum fluorides, $(H_3O)_2 \cdot [Hgua]_{16} \cdot (Al_4F_{18})_3 \cdot H_2O$ and $[Hgua]_2 \cdot (Al_5F_{17})$, are evidenced in the composition space diagram of the $Al(OH)_3$−*Hgua*Cl−HF_{aq}−EtOH system at 190 °C.

In $(H_3O)_2 \cdot [Hgua]_{16} \cdot (Al_4F_{18})_3 \cdot H_2O$, the association of four AlF_6 octahedra by vertices leads to $(Al_4F_{18})^{6-}$ entities with a −4 tetrahedral symmetry. The Al−F distances (Table 3) range Al1−F2 distance. The structure is builtup from Al_5F_{17} layers, shifted by the translation of the C-centered lattice. These (100) layers, resulting from the intergrowth of HTB and perovskite columns, are separated by guanidinium cations (Figure 6). The $CN_3H_6^+$ cations lie in (001) planes perpendicular to the inorganic Al_5F_{17} sheets.

Conclusion

This work presents a composition space diagram in the $Al(OH)_3$−*Hgua*Cl−HF_{aq}−EtOH chemical system established from microwave-heating-assisted solvothermal synthesis. The most important feature of this diagram is the first

(33) Ben Ali, A.; Body, M.; Leblanc, M.; Maisonneuve, V. *Solid State Sci.* **2010**, to be published.
(34) Gerrard, L. A.; Weller, M. T. *Chem. Mater.* **2004**, *16*, 1650.
(35) Lightfoot, P.; Stephens, N. F. *Mater. Res. Soc. Symp. Proc.* **2005**, 848.
(36) Stephens, N. F.; Lightfoot, P. *J. Solid State Chem.* **2007**, *180*, 260.
(37) Gerasimenko, A. V.; Bukvetskii, B. V.; Logvinova, V. B.; Davidovich, R. L. *Koord. Khim.* **1996**, *22*, 584.

observation of Al_5F_{17} layers in [H*gua*]$_2\cdot(Al_5F_{17})$. This phase is the second example of a hybrid fluoroaluminate after [H*py*]$\cdot(Al_3F_{10})$[22] with a 2D inorganic sublattice. This work demonstrates that the interesting region of the space diagram to obtain dense hybrid fluoroaluminates is located around the composition 25:10:65 $Al(OH)_3-$H*gua*Cl$-HF_{aq}$.

Acknowledgment. The authors thank Dr. N. Chigarev and D. Mounier (ENSIM, Le Mans, France) for the SHG test and L. Straver (Bruker AXS, Delft, The Netherlands) for the single-crystal data collection of $(H_3O)_2\cdot$[H*gua*]$_{16}\cdot(Al_4F_{18})_3\cdot H_2O$.

Supporting Information Available: Atomic coordinates, anisotropic thermal displacement parameters, main hydrogen bond distances, and X-ray crystallographic data in CIF format. This material is available free of charge via the Internet at http://pubs.acs.org.